Physica D 238 (2009) 126–136

Contents lists available at ScienceDirect

Physica D

journal homepage: www.elsevier.com/locate/physd

Multistable solitons in higher-dimensional cubic–quintic nonlinear Schrödinger lattices

C. Chong [a,*], R. Carretero-González [b], B.A. Malomed [c], P.G. Kevrekidis [d]

[a] Institut für Analysis, Dynamik und Modellierung, Universität Stuttgart, Stuttgart 70178, Germany

[b] Nonlinear Dynamical Systems Group,[1] Computational Science Research Center, and Department of Mathematics and Statistics, San Diego State University, San Diego, CA 92182-7720, USA

[c] Department of Physical Electronics, Faculty of Engineering, Tel Aviv University, Tel Aviv 69978, Israel

[d] Department of Mathematics and Statistics, University of Massachusetts, Amherst MA, 01003-4515, USA

ARTICLE INFO

Article history:
Received 9 April 2008
Received in revised form
14 September 2008
Accepted 1 October 2008
Available online 15 October 2008
Communicated by S. Kai

PACS:
52.35.Mw
42.65.-k
05.45.a
52.35.Sb

Keywords:
Nonlinear Schrödinger equation
Solitons
Bifurcations
Nonlinear lattices
Higher-dimensional

ABSTRACT

We study the existence, stability, and mobility of fundamental discrete solitons in two- and three-dimensional nonlinear Schrödinger lattices with a combination of cubic self-focusing and quintic self-defocusing onsite nonlinearities. Several species of stationary solutions are constructed, and bifurcations linking their families are investigated using parameter continuation starting from the anti-continuum limit, and also with the help of a variational approximation. In particular, a species of hybrid solitons, intermediate between the site- and bond-centered types of the localized states (with no counterpart in the 1D model), is analyzed in 2D and 3D lattices. We also discuss the mobility of multi-dimensional discrete solitons that can be set in motion by lending them kinetic energy exceeding the appropriately defined Peierls–Nabarro barrier; however, they eventually come to a halt, due to radiation loss.

1. Introduction

A large number of models relevant to various fields of physics are based on discrete nonlinear Schrödinger (DNLS) equations [1]. A realization of the one-dimensional (1D) DNLS model in arrays of parallel optical waveguides was predicted in Ref. [2], and later demonstrated experimentally, using an array mounted on a common substrate [3]. Multi-channel waveguiding systems can also be created as photonic lattices in bulk photorefractive crystals [4]. Discrete solitons are fundamental self-supporting modes in the DNLS system [1]. The mobility [5,6] and collisions [6,7] of discrete solitons have been studied in 1D systems of the DNLS type with the simplest self-focusing cubic (Kerr) nonlinearity. The DNLS equation with the cubic onsite nonlinearity is also a relevant model for Bose–Einstein condensates (BECs) trapped in deep optical lattices [8].

A more general discrete cubic nonlinearity appears in the Salerno model [9], which combines the onsite cubic terms and nonlinear coupling between adjacent sites. A modification of the Salerno model, with opposite signs in front of the onsite and inter-site cubic terms, makes it possible to study the competition between self-focusing and defocusing discrete nonlinearities of the same (third) power. This has been done in both 1D [10] and 2D [11] settings.

Lattice models with saturable onsite nonlinear terms have been studied too. The first model of that type was introduced by Vinetskii and Kukhtarev in 1975 [12]. Bright solitons in this model were predicted in 1D [13] and 2D [14] geometries. Lattice solitons supported by saturable self-defocusing nonlinearity were created in an experiment conducted in an array of optical waveguides built in a photovoltaic medium [15]. Dark discrete solitons were also

* Corresponding author.
E-mail address: christopher.chong@mathematik.uni-stuttgart.de (C. Chong).
URL: http://www.iadm.uni-stuttgart.de/LstAnaMod/Chong/home.html (C. Chong).

[1] URL: http://nlds.sdsu.edu/.

0167-2789/$ – see front matter © 2008 Elsevier B.V. All rights reserved.
doi:10.1016/j.physd.2008.10.002

considered experimentally [16] and theoretically [17] in the latter model.

Experimental observations of optical nonlinearities that may be fitted by a combination of self-focusing cubic and self-defocusing quintic terms have been reported in homogeneous [18] and heterogeneous (colloidal) [19] media (in fact, other combinations of signs of the cubic and quintic terms are possible too [19]). These observations underscore the relevance of the dynamics of solitons in the NLS equation with the cubic–quintic (CQ) nonlinearity. A family of stable exact soliton solutions to the 1D continuum NLS equation of this type is well known [20]. The possibility of building an array of parallel waveguides using optical materials with the CQ nonlinearity suggests considering the DNLS equation with the onsite nonlinearity of the CQ type. In particular, this DNLS equation arises as a limit case of the continuum CQ–NLS equation which includes a periodic potential in the form of periodic array of rectangular channels, i.e., the Kronig–Penney lattice. Families of stable bright solitons were found in 1D [21] and 2D [22] versions of the latter model (the 2D one, based on a "checkerboard" potential, supports both fundamental and vortical solitons).

The findings of a CQ–DNLS model may also be relevant in terms of the mean-field description of a self-attractive BECs confined by a slab-shaped trap, combined with a sufficiently strong 2D optical-lattice potential acting in the plane of the slab (although quantum effects, such as a superfluid to Mott insulator transition, are also relevant in the latter case [23]). The condensate trapped in each elongated potential well of this configuration is described by the Gross–Pitaevskii equation with an extra self-attractive quintic term which accounts for the deviation of the well's shape from one-dimensionality [24]. The tunneling of atoms between adjacent potential wells in this setting is approximated by the linear coupling between sites of the respective lattice.

The simplest stationary bright solitons, of the *unstaggered* type (without spatial oscillations in the solitons' tails), have been studied in the 1D version of the CQ–DNLS model in Ref. [25]. It was demonstrated that this class of solitons includes infinitely many families with distinct symmetries. The stability of the basic families was analyzed, and bifurcations between them were explored in a numerical form, and by means of a variational approximation. Dark solitons in the same model were recently studied [26] and, in another very recent work, staggered 1D bright solitons as well as the mobility of unstaggered ones have been investigated [27].

The aim of the present work is to study the existence, stability, and mobility of bright discrete solitons in two- and three-dimensional (2D and 3D) NLS lattices with the nonlinearity of the CQ type. As suggested by previous works, especially Ref. [25], the competition of the self-focusing cubic and self-defocusing quintic nonlinearities in the setting of the discrete model may readily give rise to multi-stability of discrete solitons, which is not possible in the ordinary cubic DNLS model [28], nor in the discrete CQ model where both nonlinear terms are self-focusing [29]. In addition to that, one may expect that the CQ model shares many features with those including saturable nonlinearity [30,14], such as enhanced mobility of multidimensional discrete solitons (as mentioned above, mobile discrete solitons can be readily found in the 1D CQ–DNLS equation [27]).

The paper is organized as follows. In the next section, we introduce the model and outline the method used to construct the multi-dimensional discrete solitons. In Section 3, we focus on stability and existence regions for 2D discrete solitons, and the respective bifurcations. Mobility of the 2D solitons on the lattice is studied in Section 4. Section 5 reports extensions of these results to 3D latices. In Section 6 we report analytical results obtained by means of a variational approximation, and Section 7 concludes the paper.

2. The model

In dimensionless form, the 2D DNLS equation with the onsite nonlinearity of the CQ type is:

$$\mathrm{i}\dot{\psi}_{n,m} + C\Delta^{(2)}\psi_{n,m} + 2|\psi_{n,m}|^2\psi_{n,m} - |\psi_{n,m}|^4\psi_{n,m} = 0, \tag{1}$$

where $\psi_{n,m}$ is the complex field at site $\{n, m\}$ (the amplitude of the electromagnetic field in an optical fiber, or the local mean-field wave function in BEC), $\dot{\psi} \equiv \mathrm{d}\psi/\mathrm{d}t$, and $C > 0$ is the coupling constant of the lattice model. We assume an isotropic medium, hence the discrete Laplacian is taken as

$$\Delta^{(2)}\psi_{n,m} \equiv \psi_{n+1,m} + \psi_{n-1,m} + \psi_{n,m+1} + \psi_{n,m-1} - 4\psi_{n,m}. \tag{2}$$

The CQ nonlinearity is represented by the last two terms in Eq. (1).

Eq. (1) conserves two dynamical invariants: norm (or power, in terms of optics),

$$M = \sum_{n,m} \left|\psi_{n,m}\right|^2, \tag{3}$$

and energy (Hamiltonian),

$$H = \sum_{n,m} \Big[C(|\psi_{n+1,m} - \psi_{n,m}|^2 + |\psi_{n,m+1} - \psi_{n,m}|^2) - |\psi_{n,m}|^4 + \frac{1}{3}|\psi_{n,m}|^6 \Big]. \tag{4}$$

The conserved quantities play an important role in the analysis of the mobility of discrete solitons, see Section 4.

Steady state solutions are sought for in the usual form, $\psi_{n,m} = u_{n,m}\exp(-\mathrm{i}\mu t)$, where μ is the real frequency, and the real stationary lattice field $u_{n,m}$ satisfies the following discrete equation:

$$\mu u_{n,m} + C\Delta^{(2)}u_{n,m} + 2u_{n,m}^3 - u_{n,m}^5 = 0. \tag{5}$$

More general solutions carrying topological charge, for which the stationary field $u_{n,m}$ is complex, fall outside of the scope of the present work, and will be considered elsewhere.

In one dimension, bright-soliton solutions of Eq. (5) can be found as homoclinic orbits of the corresponding two-dimensional discrete map [31]. This technique was used to construct 1D soliton solutions to the CQ–DNLS model in Ref. [25]. Since this method is not available in higher dimensions, we construct the solutions starting from the anti-continuum limit, $C \to 0$, and perform parameter continuation to $C > 0$. A multidimensional version of the variational approximation can also be used to construct solutions for small values of C, see Section 6.

In Ref. [25], two fundamental types of solutions were studied: site-centered and bond-centered solitons. Each family of solutions was further subdivided into two sub-families, which represent "tall" and "short" solutions for given parameter values. Moreover, each sub-family contains, depending on the value of C, wider solutions that may be built by appending extra excited sites to the soliton. The reason for the co-existence of the tall and short sub-families is clearly seen in the anti-continuum. If $C = 0$, Eq. (5) reduces to the following algebraic equation:

$$\mu u_{n,m} + 2u_{n,m}^3 - u_{n,m}^5 = 0, \tag{6}$$

which has at most five real solutions, *viz.*, four nontrivial ones,

$$u_{n,m} = \pm\sqrt{1 \pm \sqrt{1+\mu}}, \tag{7}$$

and $u_{n,m} = 0$ (note that these are also fixed points of the above-mentioned discrete map in the 1D case). Obviously, Eq. (7) gives, at most, two different non-trivial amplitudes, that may be continued to $C > 0$, giving rise to tall and short solitons respectively. To build

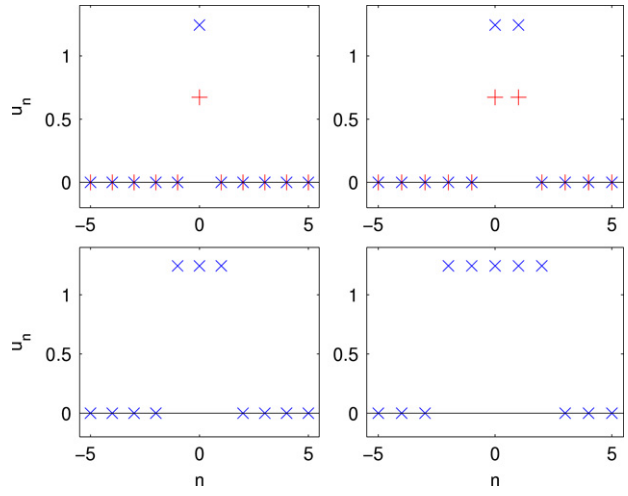

Fig. 1. (Color online) Solutions to Eq. (1) for $(\mu, C) = (-0.7, 0)$, which are used as seeds to find nontrivial solutions at $C > 0$ (only a 1D slice is shown, see Fig. 3 for profiles in two dimensions). Top left: "Tall" (blue cross markers) and "short" (red plus markers) site-centered solutions. Top right: "Tall" and "short" bond-centered solutions. Bottom: Wider extensions of the "tall" site-centered solution.

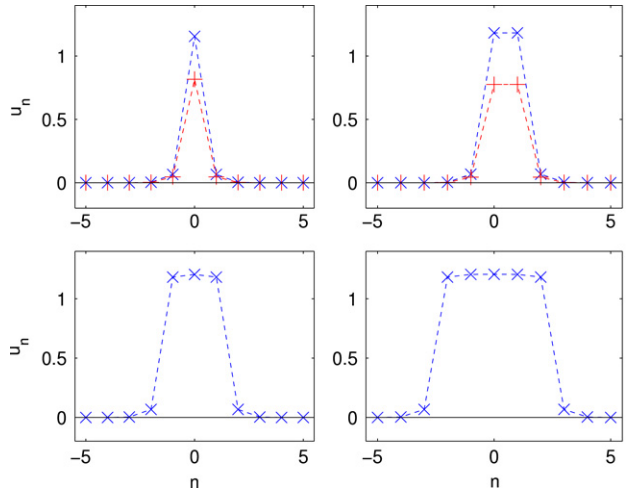

Fig. 2. (Color online) The continuation to $C = 0.1$ of the solutions shown in Fig. 1.

wider solutions, one has to consider multiple contiguous sites with nonzero field. Using the $C = 0$ solutions as seeds, we are able to generate a large family of solutions in the (μ, C) parameter plane, as shown in Figs. 1 and 2. It is found that all the wide solutions tend to disappear through saddle-node collisions between the tall and short solutions as C increases, similarly to what is the case for the cubic DNLS problem, as discussed in Ref. [32].

Another fundamental type of solution that arises in higher-dimensional lattices is a hybrid between the site-centered and the bond-centered solutions along the two spatial directions, see bottom panels in Fig. 3. This type of hybrid solution was considered previously in the case of the cubic DNLS model in Ref. [33]. We only consider these three symmetric types of localized states, namely the bond-centered, site-centered, and hybrid ones (see Fig. 3), together with their intermediate asymmetric counterparts (see Fig. 8(c) for an example). The hybrid solution admits other natural variations, namely any combination of the various types of bond-centered solutions along one axis and any site-centered profile along the other. Since their behaviors are very similar, we consider only one such type of solutions.

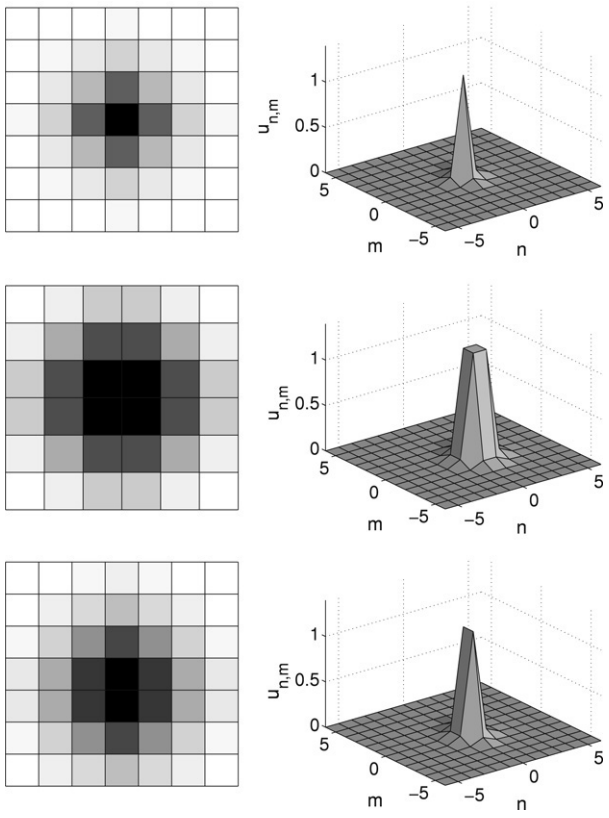

Fig. 3. Left (from top to bottom): Contour plots of solutions of the site-centered, bond-centered, and hybrid types for $(\mu, C) = (-0.7, 0.1)$. Right: The corresponding 3D plots.

3. The existence and stability of stationary solutions

Detailed existence and stability regions of all above-mentioned solutions are quite intricate and particularly hard to detect. As described for the 1D case in Ref. [25] and mentioned above, we expect in the 2D case the existence of a large family of solutions at low values of C, which gradually annihilate, through a series of bifurcations, as $C \to \infty$ (see Ref. [32] for a detailed description of the termination scenario, typically through saddle-node or pitchfork bifurcations, for the various families of the basic discrete solitons as the coupling parameter is increased). By plotting the power M for various types of the solutions (site-centered, bond-centered, and hybrid, each with various widths) at fixed values of C against frequency μ, it is possible to trace the trend followed by the solutions (see Fig. 4). For $C = 0$, the exact power for each solution can be found. A snake like pattern extending from $\mu = -1$ to $\mu = 0$ exists and continues for arbitrarily large powers. This "snaking" is also displayed for different values of $C > 0$ in Fig. 4. Branches of the $M(\mu)$ curve with higher powers correspond to wider solutions. A typical progression observed as one follows the $M(\mu)$ curve from bottom (low power) to top (high power) is switching between short and tall solutions with gradually increasing width. For example, the first branch, which represents short narrow solutions, collides with a branch of tall narrow solutions, which then collides with a set of short wide solutions, and so on. As the coupling strength increases, the power curve gets stretched upward. Following the stretching, the solutions gradually vanish, until there remains a single profile. Similar to what was found in cubic DNLS equation in Ref. [34] the bright stationary solutions in the CQ model also bifurcate from plane waves (near $\mu \approx 0$ for the CQ model). It is worthwhile highlighting here the increased level of complexity of the $M(\mu)$ curves in the cubic–quintic model (due to the interplay of short

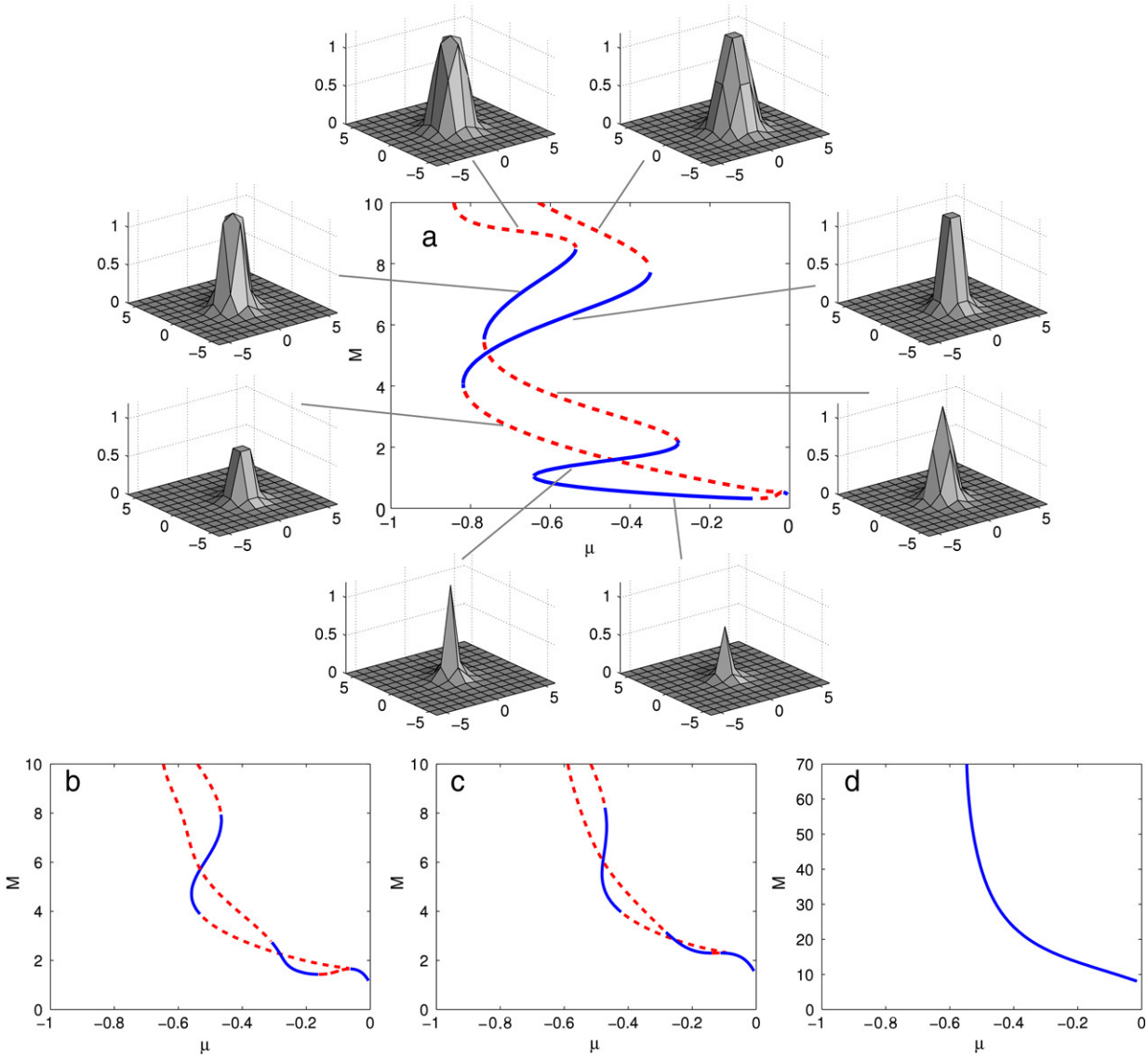

Fig. 4. (Color online) (a) Power (M) versus μ for $C = 0.1$, and respective profiles. Bottom (from left to right): Power diagrams, for (b) $C = 0.3$, (c) $C = 0.4$, and (d) $C = 2.0$, of the bond-centered and site-centered solutions. For low values of C the co-existence of multiple solutions at different values of μ is obvious. The "snaking" pattern gets stretched as C increases, slowly diminishing the number of solutions until a single solution is left. Stable and unstable solutions are represented by solid blue and dashed red curves, respectively.

and tall solution branches) in comparison to its cubic counterpart of Ref. [33], which features a single change of monotonicity (and correspondingly of stability) between narrow and tall (stable) and wide and short (unstable) solutions.

Ref. [34] provides heuristic arguments for the existence of energy thresholds for a large class of discrete systems with dimension higher than some critical value. This claim was proved in Ref. [35] for DNLS models with the nonlinearities of the form $|\psi_n|^{2\sigma+1}\psi_n$ and for a system of coupled NLS equations. As can be discerned in Fig. 4, such thresholds also exist in the case of the cubic–quintic nonlinearity.

In Ref. [25] a stability diagram for the discrete solitons in the 1D model was presented in the (μ, C) plane, which gave a clear overview of the situation. However, in the present situation, the $M(\mu)$ curves for various fixed values of C, such as those displayed in Fig. 4, provide for a better understanding of the relationships between different solutions. For example, in the (μ, C) diagram, it would appear that the taller solutions cease to exist at $(\mu, C) \approx (-0.6, 0.4)$. However, the respective $M(\mu)$ curve shows that narrow and wide solitons become indistinguishable at this point, and deciding which solution, short or tall, is annihilated becomes quite arbitrary.

A numerical linear stability analysis was performed in the usual way (see Ref. [25] for details) to investigate the stability of each of the solution branches. As one follows a $M(\mu)$ curve from bottom to top, the stability is typically swapped around each turning point, as seen in Fig. 4. However, the stability is not switched exactly at these points, as this happens via asymmetric solutions (see below).

Similar to the 1D model, a pitchfork-like bifurcation occurs between the site- and bond-centered discrete solitons. This is more clearly seen in Fig. 5. For $C = 0.5$, the bond-centered solution loses its stability in a neighborhood of $\mu \approx -0.53$, and asymmetric solutions are created there. There are multiple asymmetric solutions in this case, but only one curve appears in Fig. 5, since each one is just a rotation of the other, hence they have the same power. The bond-centered solution loses its stability before the site-centered solution regains its stability; in fact, the site-centered soliton regains the stability exactly when the asymmetric solutions collide with it. This sort of stability exchange occurs throughout the $M(\mu)$ curve. The top panel of Fig. 5 shows

Fig. 5. (Color online) Top: Pitchfork bifurcations of the bond-centered solutions and site-centered solutions for lattice coupling constant $C = 0.5$. Hybrid solutions are omitted here for clarity. Bottom: Zoom of the bifurcation scenario depicted by the rectangular region in the top panel.

Fig. 6. (Color online) Top: Bifurcations for $C = 0.4$ showing that all three fundamental modes (site-centered, bond-centered, and hybrid) are connected to each other via stability exchange with asymmetric solutions. Two asymmetric solutions are created where the bond-centered solution loses stability at the bifurcation point labeled by '**a**' in the diagram. One of these asymmetric solutions is connected to the hybrid solution at '**b**' and the other is connected to the site-centered solution at point '**c**'. A third type of asymmetric solution also emanates from the bifurcation point '**c**' which is connected to the hybrid solution at '**d**'. Bottom: The four smallest-magnitude eigenvalues of each solution corresponding to the bifurcation labeled '**a**' in the top panel. Each asymmetric solution (red dashed lines and blue dashed lines) has two branches, one positive and one negative. The bond-centered branch (green solid line) changes sign where the asymmetric branches are created showing that the bifurcation is of the pitchfork type.

two such bifurcations, with a zoom of one of them shown in the bottom panel.

The top panel of Fig. 6 shows again a site-centered solution connected to a bond-centered solution but also features a connection of the site- and bond-centered solutions via a *hybrid* solution. So not only are all variations (tall, short, narrow, etc.) within each mode connected, as shown by the snake like power curves, but all the fundamental modes (bond-centered, site-centered, hybrid) are also connected. The bottom panel of Fig. 6 shows the relevant eigenvalues corresponding to the bifurcation labeled '**a**' in the top panel. The square of the eigenvalue is shown, so that negative values correspond to stability (purely imaginary eigenvalue) and positive to instability (pairs of opposite signed real eigenvalues). For values of μ less than the bifurcation point $\mu \approx -0.415$ the bond-centered solution is stable. However, as the bifurcation point is approached, a *double* pair of eigenvalues of this bond-centered solution approaches the origin. As the instability threshold is crossed, two new branches of solutions emerge through a non-standard pitchfork bifurcation scenario. The two bifurcating branches of asymmetric solutions are represented by dashed lines, indicating their instability. This is because of the double multiplicity of the relevant eigenvalue pair (of the bond-centered solution) which leads, for each of the newly arising branches, to a splitting to one real and one imaginary pair, as is clearly illustrated in the bottom panel of Fig. 6.

We stress that the stability regions of the above-mentioned fundamental modes are almost always disjoint in regions where they each have roughly the same power and, unlike the 1D model, the asymmetric solutions are *unstable*. These features can be seen in Figs. 5 and 6. Note that the multi-stability of symmetric solutions still occurs in this case due to the existence of arbitrarily wide solutions at fixed values of C (see Fig. 4). As a general comment, it should be noted that many of the features of the 2D cubic–quintic model (such as e.g., the existence of unstable asymmetric solutions, and their connecting the fundamental modes) can also be observed in the case of the saturable model [14], although in the present case of the cubic–quintic model, the phenomenology is even richer due to, for instance, the existence of multiple (i.e., tall and short) steady states.

4. The mobility

In one dimension, traveling solutions can be found in the form

$$\psi_n = u(n - vt)\mathrm{e}^{\mathrm{i}\mu t}, \tag{8}$$

where v is a real velocity. Substitution of this expression in the 1D DNLS model yields the following advance-delay differential equation

$$\begin{aligned} 0 = &-\mathrm{i}[v\dot{u}(z) + \mathrm{i}\mu u(z)] + 2|u(z)|^2u(z) - |u(z)|^4u(z) \\ &+ C\left[u(z+1) + u(z-1) - 2u(z)\right], \end{aligned} \tag{9}$$

where $z = n - vt$. Stationary solutions are said to be *translationally invariant* if the function $u_n = u(nh)$, where h is the lattice spacing, can be extended to a one-parameter family of continuous solutions, $u(z - s)$, of the advance-delay Eq. (9) with $v = 0$. Solutions of this type have been found in other lattice models (see Refs. [36,37] and references therein). Localized solutions with non-oscillatory tails in similar models for $v \neq 0$, have been found in Refs. [30,38] by solving a respective counterpart of Eq. (9). If translationally invariant solutions exist, then sundry modes (bond-centered, site-centered, etc.) are generated by the same continuous function $u(z - s)$, each with a corresponding value of s. The translationally invariant solutions occur (i) at *transparency points*, which are points in the parameter space where solutions exchange their stability, and (ii) if the Peierls–Nabarro (PN) barrier vanishes, the barrier being defined as the difference in energy between the site-centered and bond-centered solutions. Note that (i) and (ii) are necessary but not sufficient conditions for the existence of translationally invariant solutions. For higher-dimensional lattices, translationally invariant solutions for DNLS-like models have not been found yet. However, effectively mobile lattice solitons have been found in 2D models in regions of the parameter space where